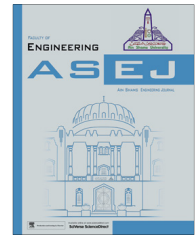




Ain Shams University  
Ain Shams Engineering Journal

[www.elsevier.com/locate/asej](http://www.elsevier.com/locate/asej)  
[www.sciencedirect.com](http://www.sciencedirect.com)



## ENGINEERING PHYSICS AND MATHEMATICS

# Pulsatile flow of couple stress fluid through a bifurcated artery

D. Srinivasacharya \*, G. Madhava Rao

*Department of Mathematics, National Institute of Technology, Warangal 506004, Telangana, India*

Received 29 December 2015; revised 30 March 2016; accepted 12 April 2016

## KEYWORDS

Blood flow;  
Pulsatile flow;  
Couple stress fluid;  
Bifurcated artery;  
Impedance

**Abstract** In the present paper, the pulsatile flow of blood through a bifurcated artery with mild stenosis in parent artery is investigated by taking blood as couple stress fluid. The arteries pattern of bifurcation is treated to be symmetric about the axis of the parent artery and straight circular cylinders of limited length. The governing equations are made dimensionless and suitable coordinate transformation is used to convert the irregular boundary to a well designed boundary. The resulting system of equations is solved numerically using the finite difference method. The influence of physical parameters on the velocity, shear stress, flow rate and impedance near the apex is studied graphically. Further, the oscillatory nature of impedance, flow rate and shear stress against time near the apex in both parent and daughter arteries is presented.

© 2016 Production and hosting by Elsevier B.V. on behalf of Ain Shams University. This is an open access article under the CC BY-NC-ND license (<http://creativecommons.org/licenses/by-nc-nd/4.0/>).

## 1. Introduction

The transport of fluids in pipes, tubes and channels is very important in many biological and biomedical systems, especially, in the human cardiovascular systems. Usually formation of fatty material such as calcium on their inner walls, is known as arterial stenosis. The deposition of atherosclerotic plaque depends on the geometry of the arteries. The most common locations of formation of stenosis are the curvatures, junctions

and bifurcations of large and medium arteries. It is important to study the bio-fluid dynamical aspects of the human cardiovascular system, which have gained more attention in the recent decades with respect to the diagnosis and the genesis of atherosclerosis.

Many researchers have studied the blood flow in stenosed arteries of different geometries. An analysis of the influence of an axially symmetric time-dependent growth of mild stenosis in the lumen of a tube whose cross section is constant through which a Newtonian fluid is flowing steadily has been described by Young [1]. The rotational field due to the spin of freely suspended particles produces an antisymmetric stress, termed as a couple-stress, which is driven to the couple stress fluid theory. Different models have been proposed to explain the behavior of non-Newtonian fluids. Among these, the micro-continuum theory of couple stress fluid introduced by Stokes [2] has specific features, such as the presence of couple stresses, body couples and non-symmetric stress tensor. The important feature of couple stresses is to introduce a size

\* Corresponding author. Tel.: +91 870 2462821; fax: +91 870 2459547.

E-mail addresses: [dsrinivasacharya@yahoo.com](mailto:dsrinivasacharya@yahoo.com), [dsc@nitw.ac.in](mailto:dsc@nitw.ac.in) (D. Srinivasacharya).

Peer review under responsibility of Ain Shams University.



Production and hosting by Elsevier

<http://dx.doi.org/10.1016/j.asej.2016.04.023>

2090-4479 © 2016 Production and hosting by Elsevier B.V. on behalf of Ain Shams University.

This is an open access article under the CC BY-NC-ND license (<http://creativecommons.org/licenses/by-nc-nd/4.0/>).

Please cite this article in press as: Srinivasacharya D, Rao GM, Pulsatile flow of couple stress fluid through a bifurcated artery, Ain Shams Eng J (2016), <http://dx.doi.org/10.1016/j.asej.2016.04.023>

dependent effect. Classical continuum mechanics oversight the size effect of material particles within the continua. Couple stress model plays a vital role in understanding some of the non-Newtonian flow properties of blood. A couple stress fluid dynamics have been reviewed by Stokes [3]. Srinivasacharya and Srikanth [4] examined the influence of couple stresses on the pulsatile nature of couple stress fluid flow through a constricted annulus and analyzed that impedance and wall shear stress have been increased with an increase in the size of the catheter and decrease in the couple stress fluid parameter. Sahu et al. [5] presented a mathematical analysis of the influence of a mild stenosis on blood flow (couple stress fluid) characteristics. Hayat et al. [6] discussed the unsteady three-dimensional flow of couple stress fluid over a stretched surface. Maiti and Misra [7] described hypothetically the peristaltic motion of a couple stress fluid in a porous channel. Srinivasacharya and Srikanth [8] investigated the steady streaming effect on the pulsatile nature of couple stress fluid. The velocity and the flow rate are increased significantly for a small increment in the couple stress parameter has been described by Adhikary and Misra [9]. The unsteady laminar incompressible flow of Eyring Powell fluid between two parallel porous plates with variable suction/injection velocity with the consideration of couple stresses and a uniform magnetic field has been discussed by Rana and Khan [10]. Reddy et al. [11] contributed to the mathematical model for couple stress fluid flow through the stenotic annular region and analyzed that the impedance has been increasing with advancing in the height and length of stenosis. Hayat et al. [12] studied the Hall effects on the peristaltic motion of couple stress fluid in an inclined asymmetric channel with heat and mass transfer. Adesanya and Makinde [13] investigated the influence of couple stress fluid flow on the steady thin flow down heated inclined plate and analyzed the effect of couple stress parameter is to cut down the flow velocity and temperature distribution. Prakash et al. [14] reported that the size of the stenoses decreases the volumetric flow rate and increases the wall shear stress as well as impedance. Makinde [15] obtained asymptotic approximations for oscillatory flow through a tube of varying cross section with permeable isothermal wall and analyzed that fluid absorption at the wall decreases the magnitude of wall shear stress, pressure drop and wall heat transfer rate, but, the influence of oscillation of the fluid is still significant at a high rate of fluid absorption at the wall. Prakash and Makinde [16] observed that the impedance is reduced due to the magnetic field effect, when patients experienced thermal radiation therapy. Sibanda

et al. [17] studied the bio-mechanics of blood flow through a slightly diverging channel. Makinde [18] investigated the laminar flow through a channel of different widths with permeable walls. A mathematical model describing the fluid dynamics of the collapsible tube has been presented by Makinde [19] and mentioned that this model is most suitable to simulate wind tunnel tests on rheological phenomenon in physiological systems.

In the above mentioned literature, the influence of bifurcation of the artery on blood flow characteristics was neglected. The pulsatile flow of an incompressible couple stress fluid through a bifurcated artery with mild stenosis is considered. All the physiological properties of blood at the bifurcation of the artery were severely influenced by different parameters. Hence, the aim of the present article was to study the couple stress fluid through a bifurcated artery with mild stenosis in the parent lumen. The variation of flow rate, impedance and shearing stress are analyzed for various values of couple stress fluid parameters and geometric parameters.

## 2. Mathematical formulation

Consider laminar, incompressible blood flow passing through a stenosed bifurcated artery. Blood is assumed as an unsteady couple stress fluid of constant density. The arteries, forming bifurcation are assumed to be straight, circular cylinders of limited length and symmetrical about the axes of the parent artery as shown in Fig. 1. Let  $(r, \theta, z)$  be any point in a cylindrical polar coordinate system, of which  $z$  is taken to be the central axis of the parent artery. To avoid the possibility of appearance of flow separation zones, introduce curvature at the lateral junction and the flow divider.

The equations governing the pulsatile couple stress fluid flow are

$$\frac{\partial \rho}{\partial t} + \rho(\nabla \cdot \mathbf{q}) = 0 \quad (1)$$

$$\rho \left( \frac{\partial \mathbf{q}}{\partial t} + (\mathbf{q} \cdot \nabla) \mathbf{q} \right) = -\nabla P + \mu(\nabla \times \nabla \times \mathbf{q}) - \eta(\nabla \times \nabla \times \nabla \times \mathbf{q}) \quad (2)$$

where  $p$  is the fluid pressure,  $\rho$  is the density of the couple stress fluid,  $\eta$  is the couple stress viscosity parameter,  $\mathbf{q}$  is the velocity vector and  $\mu$  is the blood viscosity.

The mathematical representation of bifurcated artery with mild stenosis in the parent lumen is presented by [20,21],

$$R_1(z, t) = \begin{cases} a, a_1(t) & 0 \leq z \leq d' \quad \text{and} \quad d' + l_0 \leq z \leq z_1 \\ \left( a - \frac{4c}{r_0^2} (l_0(z - d') - (z - d')^2) \right) a_1(t) & d' \leq z \leq d' + l_0 \\ \left( a + r_0 - \sqrt{r_0^2 - (z - z_1)^2} \right) a_1(t) & z_1 \leq z \leq z_2 \\ (2r_1 \sec \beta + (z - z_2) \tan \beta) a_1(t), & z_2 \leq z \leq z_{max} \end{cases} \quad (3)$$

$$R_2(z, t) = \begin{cases} 0, & 0 \leq z \leq z_3 \\ \sqrt{(r'_0)^2 - (z - z_3 - r'_0)^2} \quad b_1(t) & z_3 \leq z \leq z_3 + r'_0(1 - \sin \beta) \\ (r'_0 \cos \beta + z_4) \quad b_1(t) & z_3 + r'_0(1 - \sin \beta) \leq z \leq z_{max} \end{cases} \quad (4)$$

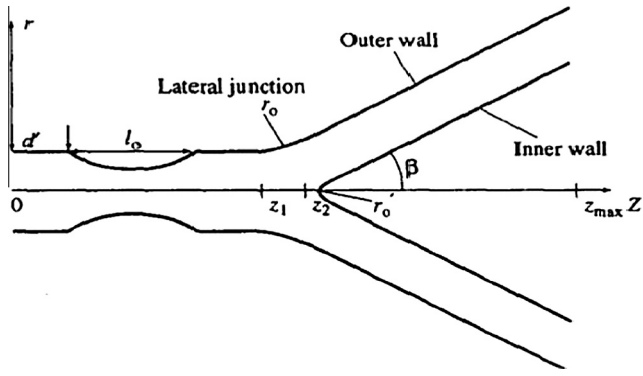


Figure 1 Schematic diagram of stenosed bifurcated artery.

where  $R_1(z, t)$  is the outer wall and  $R_2(z, t)$  is the inner wall of the bifurcated artery,  $r_1$  is the radius of the daughter artery,  $a$  is the radius of the parent artery at non-stenosed portion, and  $l_0$  is the length of the stenosis at a distance  $d'$  from the origin.  $z_1$ ,  $z_2$  and  $z_3$  are the location of the onset, offset of the lateral junction and flow divider respectively,  $\beta$  is the half of the bifurcation angle,  $\varepsilon$  is the maximum height of the stenosis at  $z = d' + l_0/2$  and  $z_{max}$  represents the maximum length of the bifurcated artery and  $a_1(t)$ ,  $b_1(t)$  are given by

$$a_1(t) = 1 - (\cos(\omega t) - 1)k \exp(-k\omega t) \text{ and } b_1(t) = 1/a_1(t) \quad (5)$$

The radii of curvature  $r_0$  and  $r'_0$  at the lateral junction and flow divider that are present in the geometry are given by

$$r_0 = \frac{a - 2r_1 \sec \beta}{\cos \beta - 1} \quad \text{and} \quad r'_0 = \frac{(z_3 - z_2) \sin \beta}{1 - \sin \beta} \quad (6)$$

where  $z_1$ ,  $z_2$  and  $z_3$  are the location of the onset, offset of the lateral junction and flow divider which lie on the central axis of the artery and are functions of the half of bifurcated angle, defined as  $z_2 = z_1 + r_0 \sin \beta$ ,  $z_3 = z_2 + q_1$ ,  $z_4 = (z - z_3 - r'_0(1 - \sin \beta)) \tan \beta$ . Here  $q_1$  is a small number lying in between 0.1 and 0.5, and this is defined in the agreement with the geometry.

Since the flow is considered to be symmetric, all the variables are independent of  $\theta$ , and the velocity is given by  $\mathbf{q} = (u(r, z, t), 0, w(r, z, t))$ . Using  $L$  is characteristic length and  $w_0$  is characteristic velocity, we define the non-dimensional variables as follows:

$$r = a\tilde{r}, \quad u = \frac{aw_0\tilde{u}}{L}, \quad z = L\tilde{z}, \quad w = w_0\tilde{w}, \quad d = L\tilde{d},$$

$$p = \frac{Lw_0\mu\tilde{p}}{a^2}, \quad R_1(z) = a\tilde{R}_1(\tilde{z}), \quad R_2(z) = a\tilde{R}_2(\tilde{z}) \quad t = \frac{\tilde{t}}{\omega}$$

It can be shown that the radial velocity is very small and can be neglected for a low Reynolds number flow in an artery with mild stenosis [4]. Therefore, Eq. (2) can be written in non-dimensional form as

$$R_w^2 \frac{\partial w}{\partial t} = -\frac{dp}{dz} + \left[ \frac{\partial^2}{\partial r^2} + \frac{1}{r} \frac{\partial}{\partial r} \right] w - \frac{1}{\alpha^2} \left[ \frac{\partial^2}{\partial r^2} + \frac{1}{r} \frac{\partial}{\partial r} \right]^2 w \quad (7)$$

where  $\alpha^2 = \frac{\mu w_0^2}{\eta}$  is the couple stress fluid parameter and  $R_w^2 = \frac{a^2 \rho \omega}{\mu}$  is the Womersley number.

The equation of the pulsatile pressure gradient in the above equation in non-dimensional form is

$$-\frac{\partial p}{\partial z} = A_0 + A_1 \cos(t) \quad (8)$$

where  $A_0$  is the amplitude of the pressure gradient (constant), and  $A_1$  is the amplitude of the pulsatile component, which is the systolic and diastolic pressure. Where  $w = 2\pi f_p$ ,  $f_p$  is the frequency of the pulsatile flow.

The boundary conditions in non-dimensional form are

$$\left. \begin{aligned} \frac{\partial w}{\partial r} &= 0, \quad \frac{\partial^2 w}{\partial r^2} - \frac{\sigma}{r} \frac{\partial w}{\partial r} = 0, \quad \text{on } r = 0 \text{ for } 0 \leq z \leq z_3 \\ w &= 0, \quad \frac{\partial^2 w}{\partial r^2} - \frac{\sigma}{r} \frac{\partial w}{\partial r} = 0, \quad \text{on } r = R_1(z) \text{ for all } z \\ w &= 0, \quad \frac{\partial^2 w}{\partial r^2} - \frac{\sigma}{r} \frac{\partial w}{\partial r} = 0, \quad \text{on } r = R_2(z) \text{ for } z_3 \leq z \leq z_{max} \\ w &= c_0 \text{ at } t = 0 \end{aligned} \right\} \quad \text{where } c_0 \text{ is very small.} \quad (9)$$

where  $\sigma = \eta/\eta'$  is the couple stress fluid parameter which is responsible for the effect of local viscosity of particles apart from the bulk viscosity of the fluid. If  $\eta = \eta'$  then the effects of couple stresses will be absent in a material, which implies that couple stress tensor is symmetric. In this case Eq. (9) shows that, the couple stresses are disappearing on the inner and outer walls of the bifurcated artery.

The influence of  $R_1$  and  $R_2$  of the boundary can be conveyed into the governing equations by the radial coordinate transformation given by Shit and Roy [22],  $\xi = (r - R_2)/R$  where  $R = R_1 - R_2$ . Using this transformation in Eq. (7) reduces the form

$$\begin{aligned} & -R_w^2 R^3 \left( \xi \frac{\partial R}{\partial t} + \frac{\partial R_2}{\partial t} \right) \frac{\partial w}{\partial \xi} + R^4 \frac{dp}{dz} + \frac{1}{\alpha^2} \frac{\partial^4 w}{\partial \xi^4} \\ & + \frac{2R}{\alpha^2 (\xi R + R_2)} \frac{\partial^3 w}{\partial \xi^3} - \left[ 1 + \frac{1}{\alpha^2 (\xi R + R_2)^2} \right] R^2 \frac{\partial^2 w}{\partial \xi^2} \\ & + \left[ \frac{1}{\alpha^2 (\xi R + R_2)^3} - \frac{1}{(\xi R + R_2)} \right] R^3 \frac{\partial w}{\partial \xi} \\ & = -R_w^2 R^4 \frac{\partial w}{\partial t} \end{aligned} \quad (10)$$

In the above equation first term is corresponding to wall motion. The associated boundary conditions in the transformed coordinates are

$$\left. \begin{aligned} \frac{\partial w}{\partial \xi} &= 0, \quad \frac{\partial^2 w}{\partial \xi^2} - \frac{\sigma R}{(\xi R + R_2)} \frac{\partial w}{\partial \xi} = 0, \quad \text{on } \xi = 0 \text{ for } 0 \leq z \leq z_3 \\ w &= 0, \quad \frac{\partial^2 w}{\partial \xi^2} - \frac{\sigma R}{(\xi R + R_2)} \frac{\partial w}{\partial \xi} = 0, \quad \text{on } \xi = 1 \text{ for all } z \\ w &= 0, \quad \frac{\partial^2 w}{\partial \xi^2} - \frac{\sigma R}{(\xi R + R_2)} \frac{\partial w}{\partial \xi} = 0, \quad \text{on } \xi = 0 \text{ for } z_3 \leq z \leq z_{max} \\ w &= \frac{c_0}{w_0} \text{ at } t = 0 \end{aligned} \right\} \quad (11)$$

### 3. Numerical solution

Eq. (10) along with the boundary conditions Eq. (11) is solved numerically using finite difference method. First, Eq. (10) is converted into a system of four first order partial differential equations and these equations are replaced with equivalent central finite difference approximations, so that the four first order equations result in a block tridiagonal matrix and then this system is solved using block elimination method.

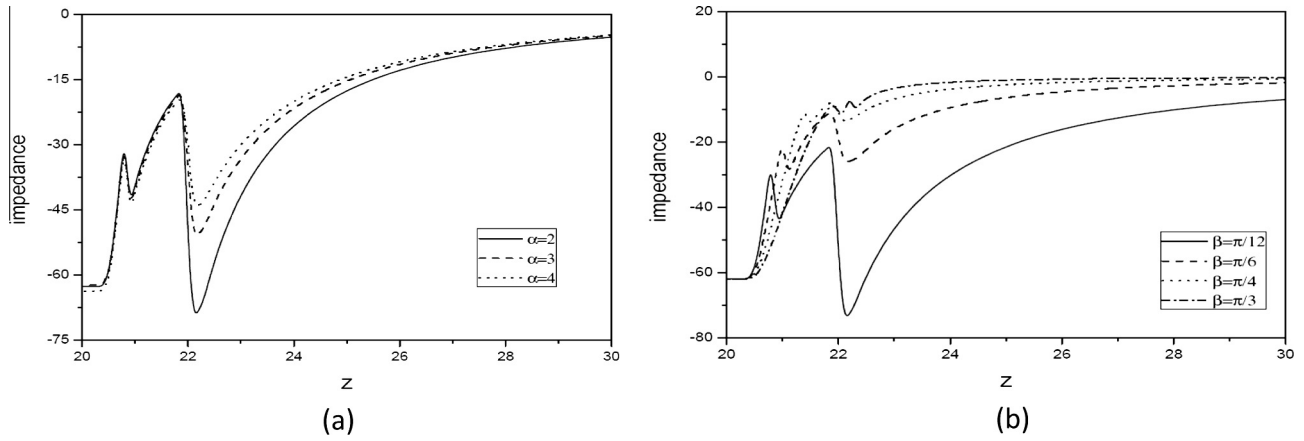


**Figure 2** Effect of (a)  $\alpha$  and (b)  $\beta$  on impedance near to the apex.

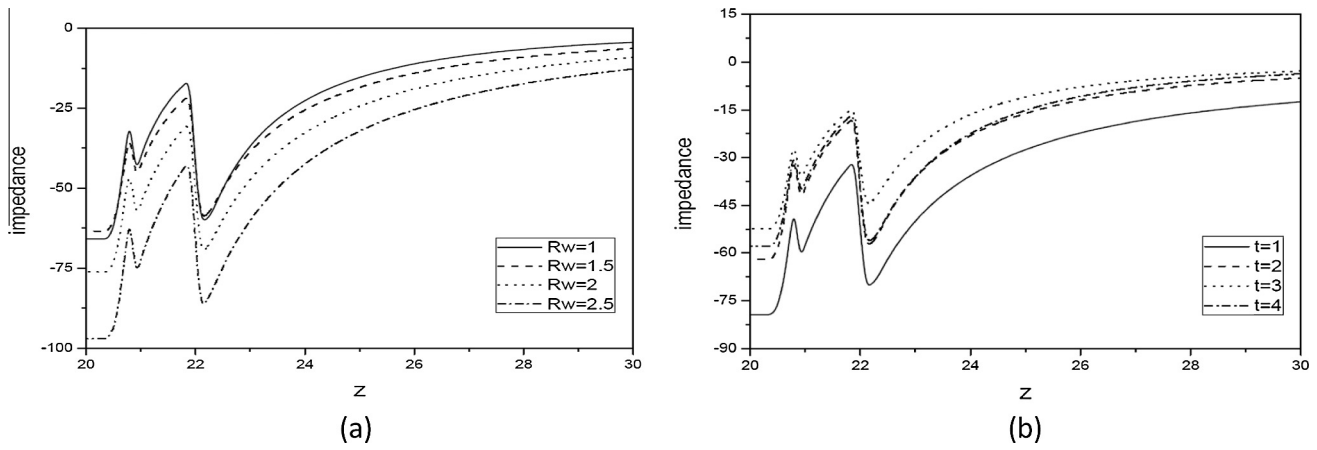


**Figure 3** Influence of (a)  $R_w$  and (b)  $t$  on impedance near to the apex.

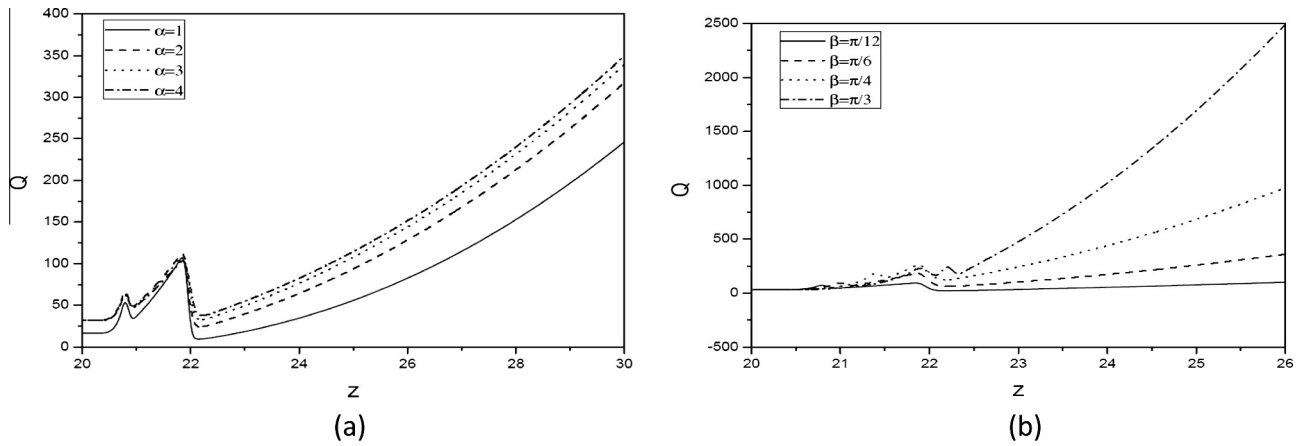


**Figure 4** Influence of (a)  $\alpha$  and (b)  $\beta$  on flow rate near to the apex.

The physical quantities to be analyzed are flow rate, impedance and shear stress for both parent and daughter arteries. The flow rate for both parent and daughter arteries is determined using

$$Q_p = 2\pi R \left[ R \int_0^1 \xi w d\xi + R_2 \int_0^1 w d\xi \right] \text{ and} \\ Q_d = \pi R \left[ R \int_0^1 \xi w d\xi + R_2 \int_0^1 w d\xi \right] \quad (12)$$

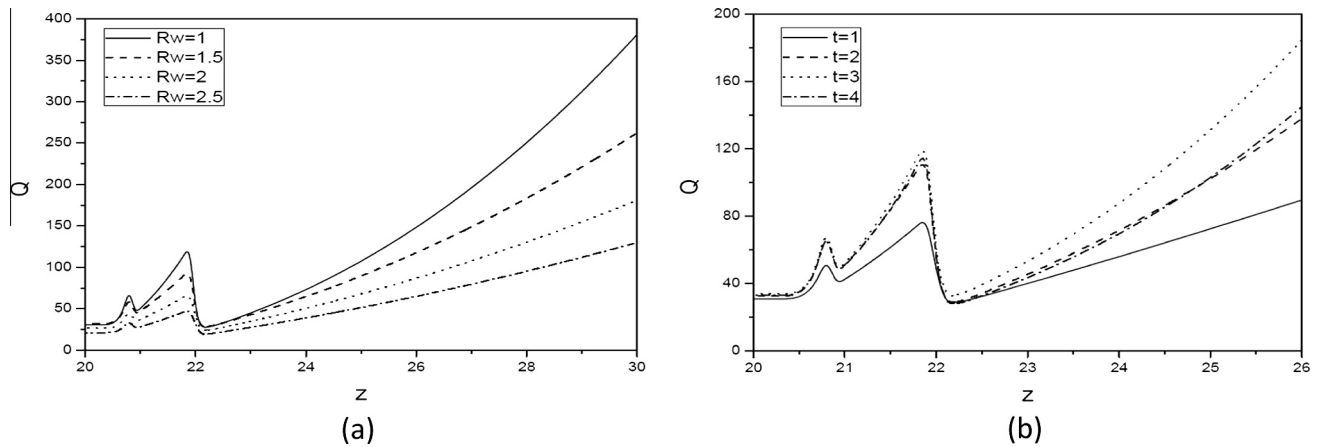


**Figure 5** Influence of (a)  $R_w$  and (b)  $t$  on flow rate near to the apex.

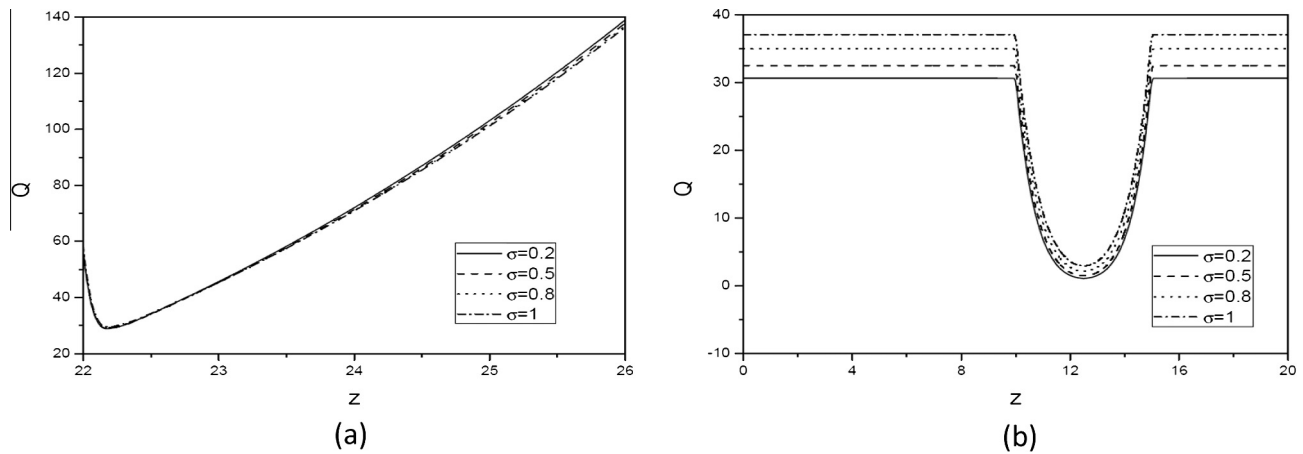


**Figure 6** Influence of  $\sigma$  in (a) daughter and (b) parent artery on flow rate near to the apex.

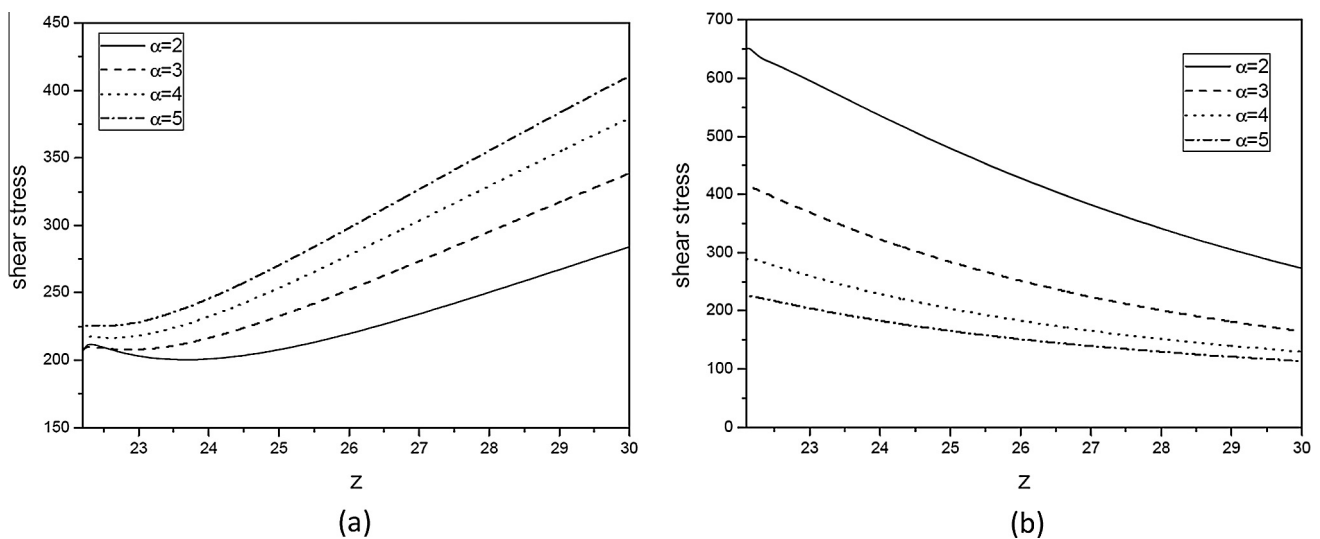


**Figure 7** Effect of  $\alpha$  on shear stress along the (a) inner and (b) outer walls of the daughter artery.

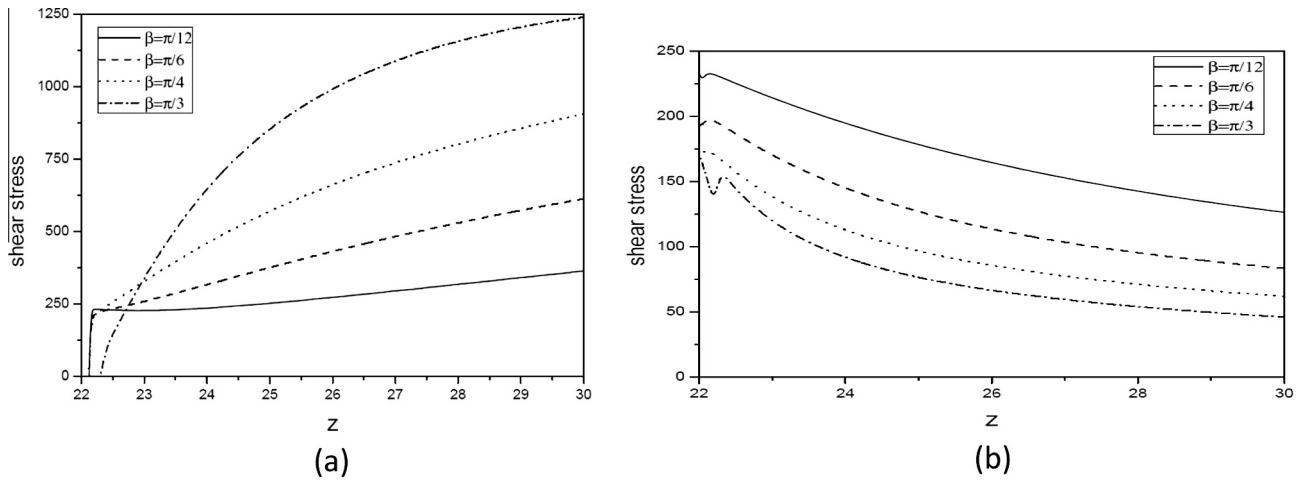


**Figure 8** Effect of  $\beta$  on shear stress along the (a) inner and (b) outer walls of the daughter artery.

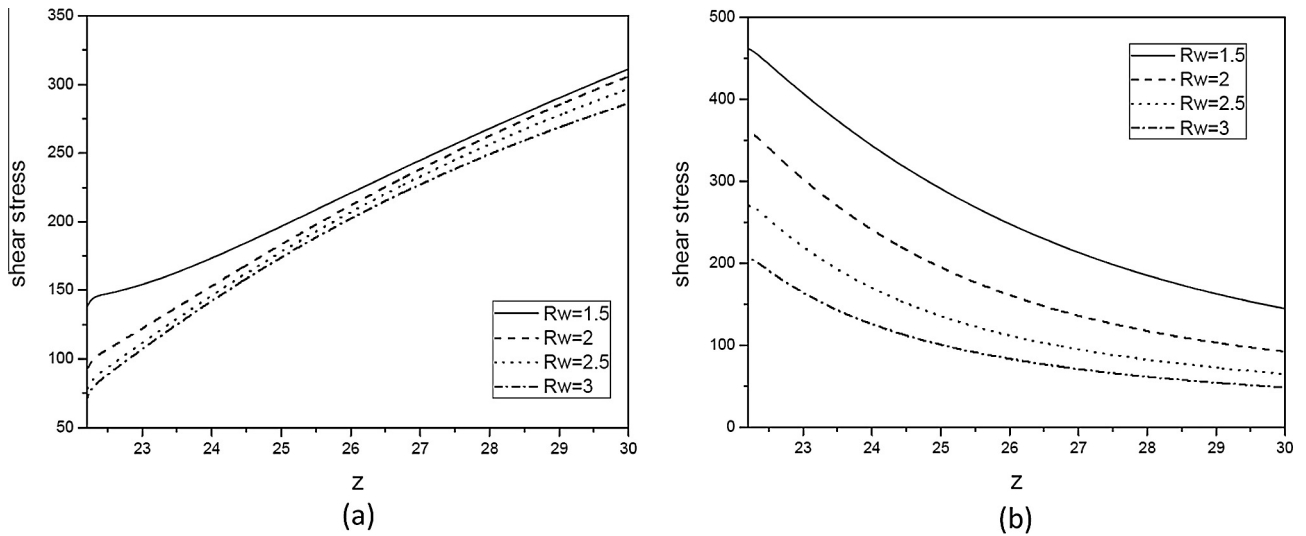


**Figure 9** Effect of  $R_w$  on shear stress along the (a) inner and (b) outer walls of the daughter artery.

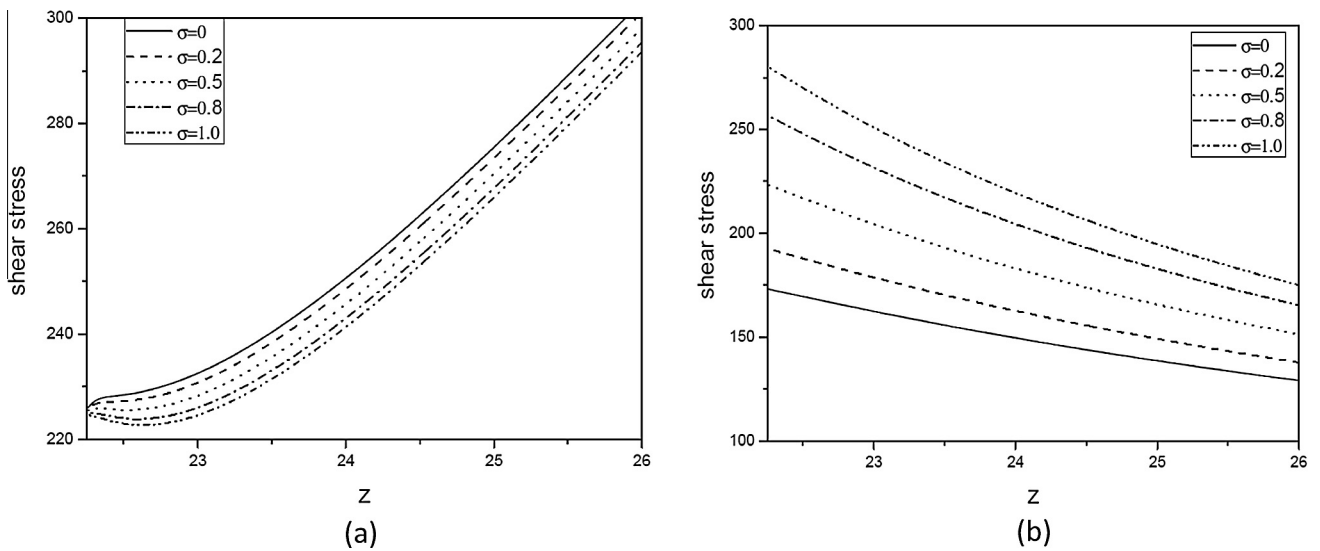


**Figure 10** Effect of  $\sigma$  on shear stress along the (a) inner and (b) outer walls of the daughter artery.



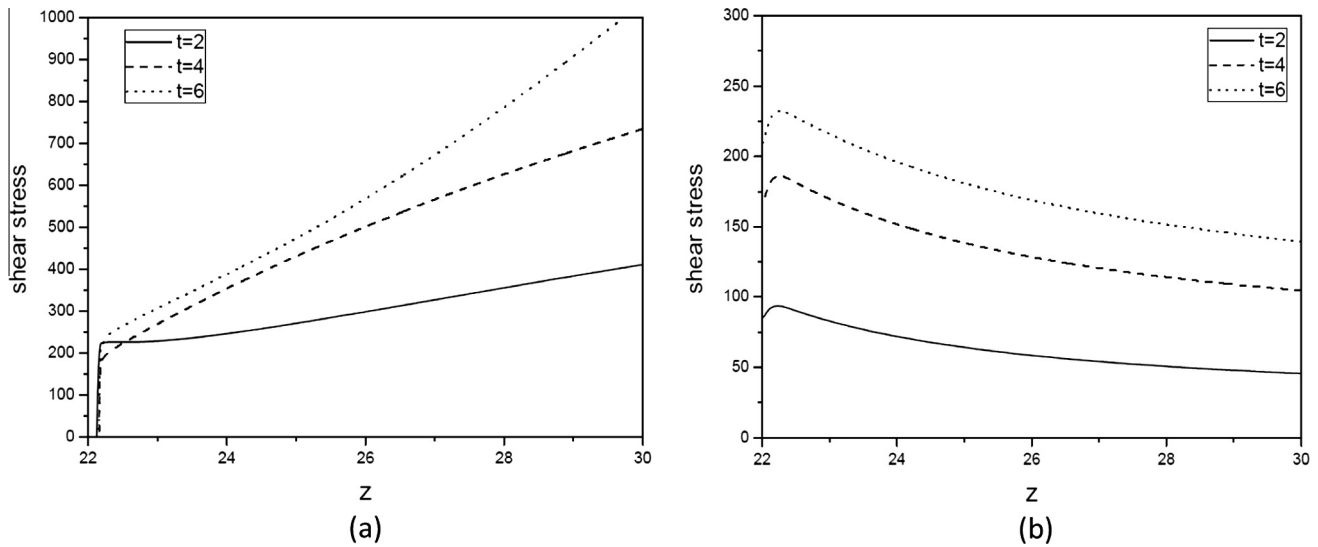


**Figure 11** Effect of  $t$  on shear stress along the (a) inner and (b) outer walls of the daughter artery.

For the impedance of the flow in the parent and daughter artery is calculated using

$$(\lambda_p)_i = \left| \frac{z_3 \frac{dp}{dz}}{Q_p} \right| \text{ for } z < z_3 \text{ and}$$

$$(\lambda_d)_i = \left| \frac{(z_{max} - z_3) \frac{dp}{dz}}{Q_d} \right| \text{ for } z \geq z_3 \quad (13)$$

The mean value of shear stress is calculated by using

$$\tau_{ij} = \frac{1}{R} \frac{\partial w}{\partial \xi} + \frac{1}{4R\alpha^2(\xi R + R_2)^2} \frac{\partial w}{\partial \xi} - \frac{1}{4\alpha^2 R^3} \frac{\partial}{\partial \xi} \left( \frac{\partial^2 w}{\partial \xi^2} \right)$$

$$- \frac{1}{4R^2\alpha^2(\xi R + R_2)} \frac{\partial^2 w}{\partial \xi^2} \quad (14)$$

#### 4. Results and discussions

The aim of the current study was to analyze the flow characteristics of blood through the stenosed bifurcated artery under the consideration that blood is pulsatile couple stress fluid. An appropriate numerical scheme has been chosen to analyze the applicability of the physiological data available in the scientific literatures. The numerical solutions of all these physical parameters are presented graphically for different values of  $\alpha$ ,  $\beta$ ,  $\sigma$  and time on both sides of the bifurcated artery for better understanding of the analysis. We used the following data  $a = 5$  mm,  $d = 10$  mm,  $l_0 = 5$  mm,  $\beta = \pi/10$ ,  $r_1 = 0.51a$ ,  $\varepsilon = 2$ ,  $\alpha = 2.5$ ,  $t = 2$  s and  $\sigma = 0.5$ .

The parameter  $l = \sqrt{\frac{\eta}{\mu}}$  is the characteristic measure of the polarity of the fluid model, and it has the dimensions of the length. If  $l$  is a function of the molecular dimensions of the

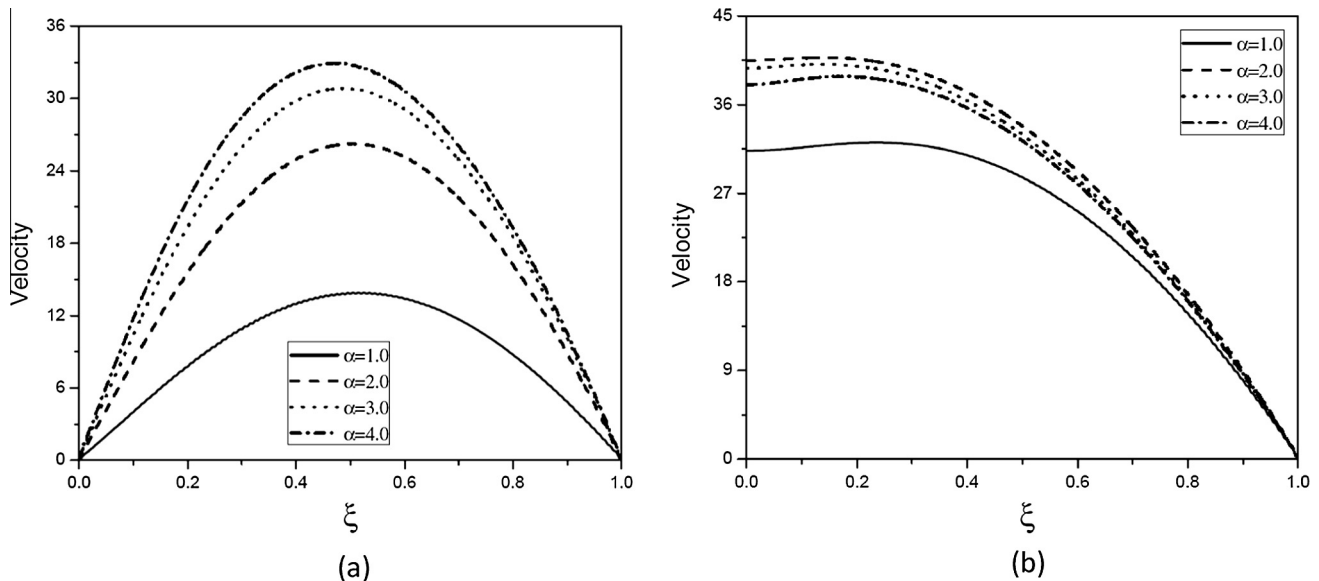


**Figure 12** Effect of  $\alpha$  on velocity near the apex in both (a) daughter and (b) parent arteries.

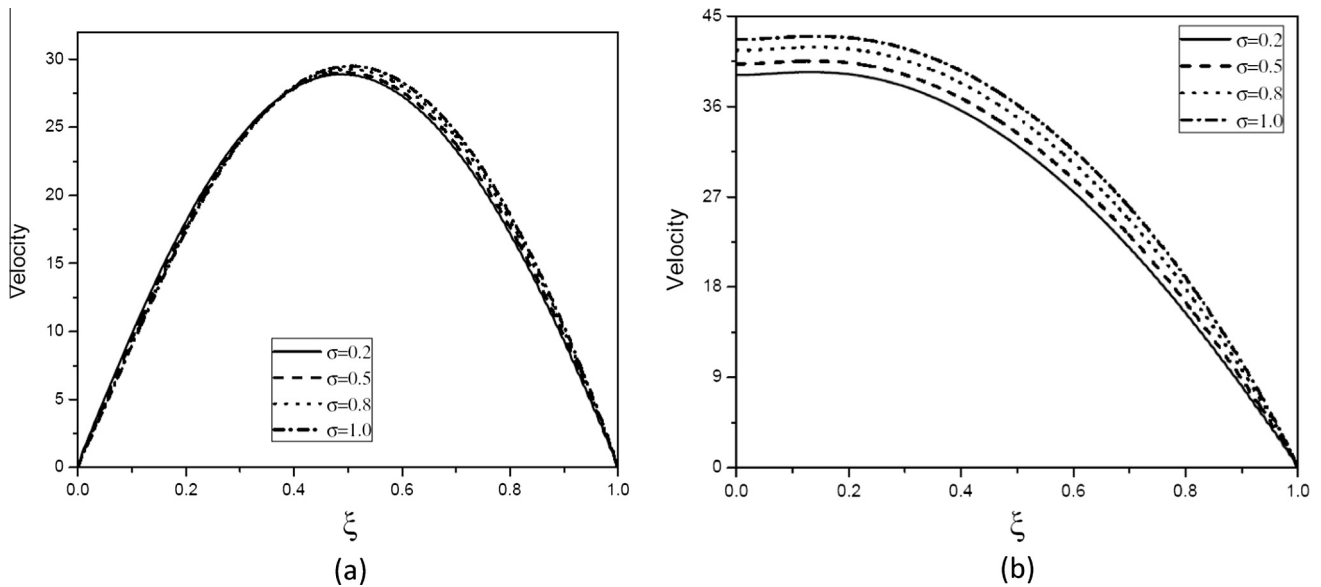


**Figure 13** Effect of  $\sigma$  on velocity near the apex in both (a) daughter and (b) parent arteries.

liquid, it will vary greatly for different liquids. For example, the length of a polymer chain may be a million times the diameter of water molecule Stokes [2]. One might therefore expect the couple stresses to appear in noticeable magnitudes in liquids with very large molecules.  $\alpha$  indicates the ratio of the tube radius to the characteristic length, i.e., ( $\alpha = a/l$ ). In the limit  $\eta \rightarrow 0$  i.e.  $\alpha \rightarrow \infty$  Eq. (2) reduces to classical Navier–Stokes equation. Hence, for larger values of  $\alpha$ , the effect of couple stresses is not significant.

The effect of  $\alpha$  and  $\beta$  on impedance in both sides of the apex is described in Fig. 2a and b. It is noticed from these figures that the resistive impedance is increasing with the increase in the value of  $\alpha$  and  $\beta$  on both sides of flow divider. The influence of  $R_w$  and  $t$  on impedance in both sides of the apex is presented in Fig. 3a and b respectively. It is observed from Fig. 3a

that the impedance is diminishing with an increase in the value of  $R_w$ . It is depicted from Fig. 3b that the impedance is increasing with the increase in the value of  $t$  on both sides of the apex. Figs. 2 and 3 show that the impedance is flustered largely near to the flow divider in the parent artery due to the presence of degeneration of flow at the start of the flow divider. All the profiles are locally rising till inset of lateral junction, and then a small decrease is identified and then rise until the flow divider. Thereafter, these profiles found to be steady till  $z_{max}$ .

The variations of flow rate on both sides of the apex with  $\alpha$  and  $\beta$  are depicted in Fig. 4a and b. From these figures it is noticed that the flow rate is enhanced with advance in the value of  $\alpha$  and  $\beta$  on both sides of the apex. Fig. 5a and b shows the effect of  $R_w$  and  $t$  on the volumetric flow rate in both sides of the apex. It is observed that the flow rate is diminishing with

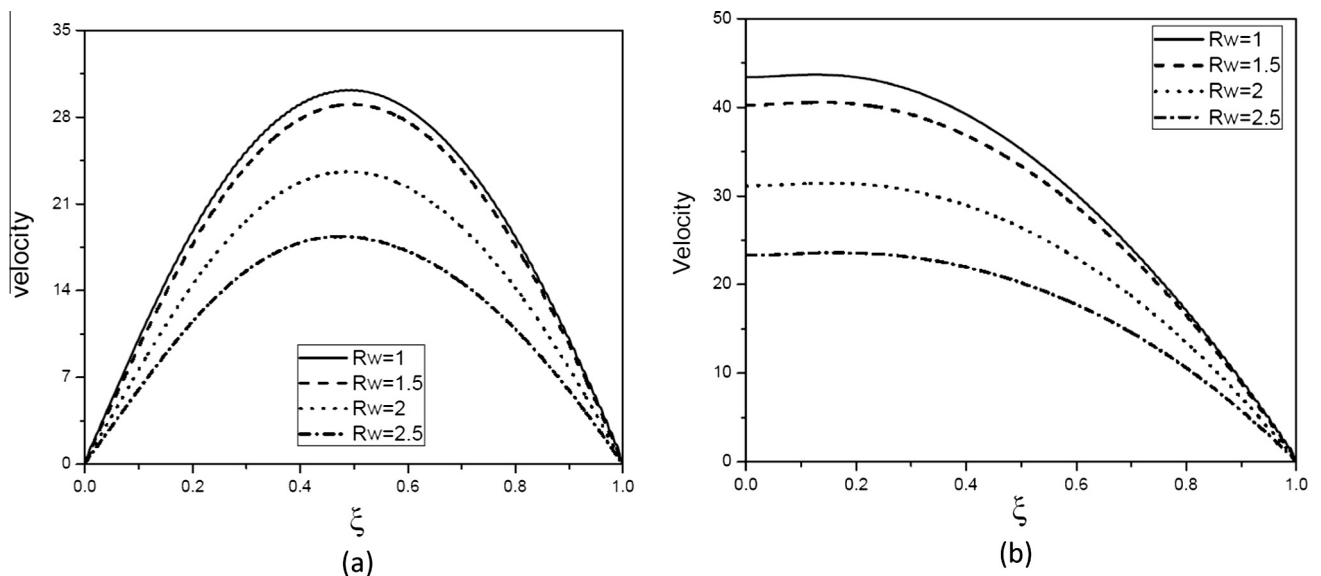


**Figure 14** Effect of  $R_w$  on velocity near the apex in both (a) daughter and (b) parent arteries.



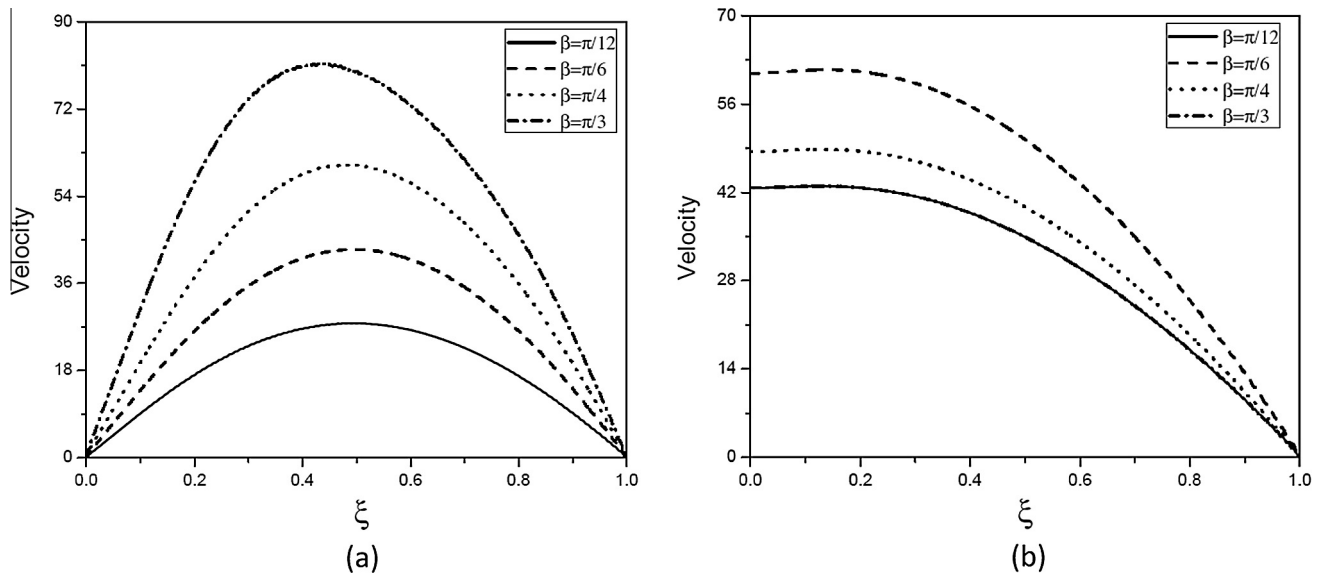


**Figure 15** Effect of  $t$  on velocity near the apex in both (a) daughter and (b) parent arteries.

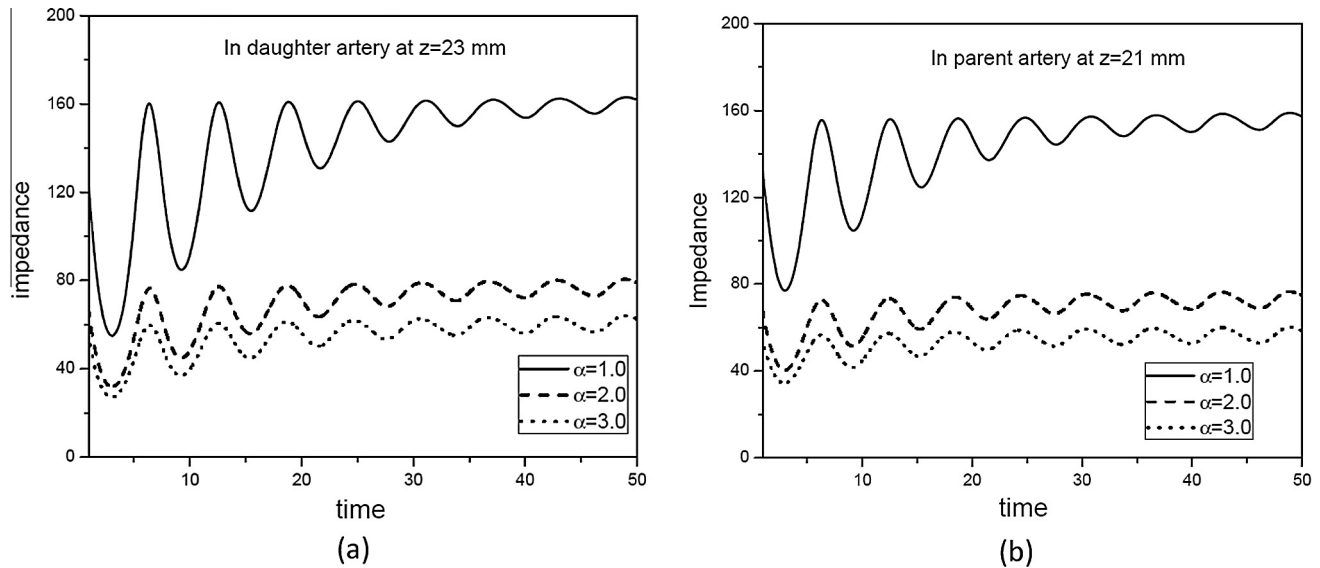


**Figure 16** Oscillatory nature of impedance against time near the apex in both (a) parent and (b) daughter arteries.

advancement in the value of  $R_w$ . It is depicted that the flow rate is advancing with advancement in the value of  $t$  on both sides of the apex. The effect of  $\sigma$  on flow rate in both daughter and parent arteries is shown in Fig. 6a and b respectively. These figures illustrate that the flow rate is increasing in parent artery and diminishing in the daughter artery with increase in the value of  $\sigma$ , but the effect is not much significant in daughter artery. The flow rate in case of couple stress fluid is less than that of Newtonian fluid in the parent artery at the maximum height of the stenosis.  $\sigma = 1$  corresponds to Newtonian fluid case, where couple stresses will disappear in the wall. It is to be noted from Figs. 4–6 that the flow rate is rising with the rise in the value of  $z$ , until inset of lateral junction; then, a slight decrease occurred suddenly, and after that gradually rising till the apex, and then a sudden decrease is identified. This is

because of diverging of blood flow at the bifurcation of the artery. Thereafter, it is found that the flow rate is uniform till  $z_{max}$ .

Fig. 7a and b explores the influence of  $\alpha$  on shear stress along the inner and outer walls of the daughter artery. From these figures it is observed that the shear stress increases along the inner wall and decreases along the outer wall of the daughter artery with an increase in the value of  $\alpha$ . Fig. 8a and b illustrates the influence of  $\beta$  on shear stress along the inner and outer walls of the daughter artery. From these figures it is noticed that the shear stress is enhancing along the inner wall and diminishing along the outer wall with an increase in the value of  $\beta$ . The influence of  $R_w$  on shear stress along the inner and outer walls of the daughter artery is presented in Fig. 9a and b. It is seen that shear stress is diminishing with

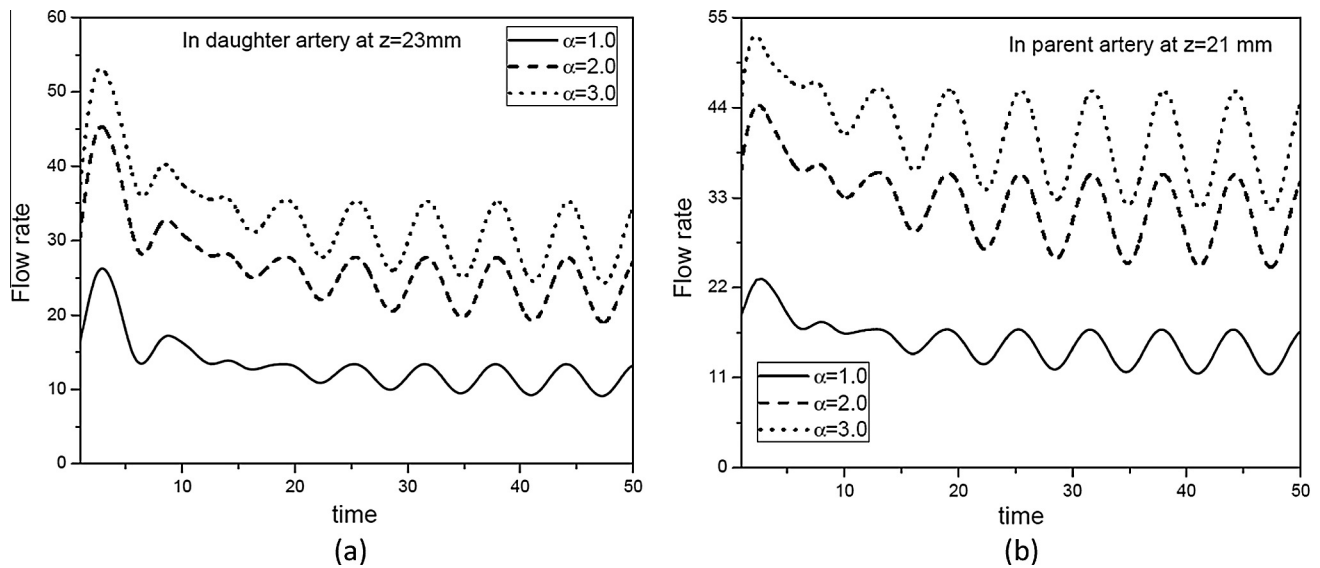


**Figure 17** Oscillatory nature of flow rate against time near the apex in both (a) parent and (b) daughter arteries.

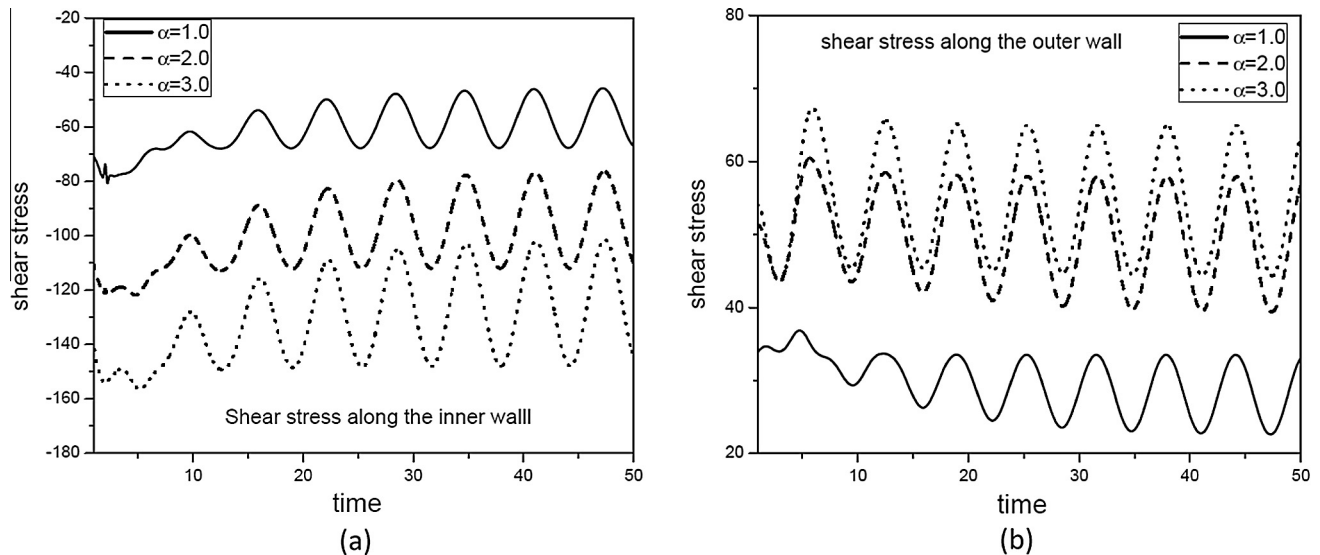


**Figure 18** Pulsatile nature of shear stress along the (a) inner and (b) outer walls of the daughter artery against time.

advancement in the value of  $R_w$  along the inner and outer walls of the daughter artery. The variations of shear stress with  $\sigma$  along the inner and outer walls of the daughter artery are presented in Fig. 10a and b. Fig. 10a illustrates that the shear stress is decreasing along the inner wall and from Fig. 10b shear stress is increased along the outer wall of the daughter artery with an increase in the value of  $\sigma$ . The variations of shear stress along the inner and outer walls of the daughter artery with time are depicted in Fig. 11a and b. From these figures it is seen that shear stress is advancing with advancement in time along both inner and outer walls of the daughter artery.

The variations of velocity with couple stress fluid parameter  $\alpha$  in both daughter and parent arteries near the apex are shown respectively in Fig. 12a and b. From these figures, it is noticed that velocity is rising with an advancement in the value of  $\alpha$  in both parent and daughter arteries. Fig. 13a and b depicts the effect of  $\sigma$  on velocity in both parent and daughter arteries

near the apex. From Fig. 13a, it is observed that the effect of  $\sigma$  on velocity is almost negligible in the daughter artery, but from Fig. 13b it is noticed that the velocity is increasing with an increase in the value of  $\sigma$  in parent artery. Fig. 14a and b respectively illustrates the influence of Womersley number on velocity near the apex in both parent and daughter arteries. From these figures, it is observed that the velocity is decreasing with an advancement in the value of  $R_w$  in both daughter and parent arteries. The effect of bifurcation angle ( $\beta$ ) on velocity in both daughter and parent arteries is reported in Fig. 15a and b. It is noticed that the velocity is rising with an advancement in the value of  $\beta$  in both parent and daughter arteries. It is worth to mention that the velocity remains constant at non-stenosed portion.

The oscillatory profiles of impedance and flow rate against time ( $t$ ) with couple stress fluid parameter ( $\alpha$ ) on both sides of the apex are presented in Figs. 16a, b and 17a and b. From

Fig. 16a and b impedance is diminishing with an increase in the value of  $\alpha$  in both parent and daughter arteries. From Fig. 17a and b flow rate is enhanced with an advancement in the value of  $\alpha$  in both parent and daughter arteries. The pulsatile nature of shear stress along the inner and outer walls of the daughter artery is shown in Fig. 18a and b. From these Fig. 18a shear stress is decreasing along the inner wall and from Fig. 18b shear stress increases along the outer wall with an increase in the value of  $\alpha$ . In Figs. 16–18 wavy graphs are shown due to pulsatile nature of the blood flow.

## 5. Conclusion

The present results make us to understand, numerically as well as physically, the influence of  $\alpha$ ,  $\beta$ ,  $\sigma$  and  $t$  on pulsatile couple stress blood flow through bifurcated artery with mild stenosis, which is of great importance in the medical sciences and diagnosis of diseases.

1. The impedance and volumetric flow rate both are increasing with the increase in the value of  $\alpha$ ,  $\beta$ ,  $t$  and decrease with the value of  $R_w$  in both parent and daughter arteries. But these profiles are increasing in the parent artery and decreasing in the daughter artery with an increase in the value of  $\sigma$ .
2. The shear stress is increasing with the increase in the value of  $\alpha$ ,  $\beta$ ,  $t$ , and decreasing with increase in the value of  $R_w$ ,  $\sigma$  along the inner wall. Also, it is increasing with an increase in the values of  $\sigma$ ,  $t$  and decrease with increase in the value of  $\alpha$ ,  $\beta$ ,  $R_w$  along the outer wall of daughter artery.
3. The velocity is increasing with the increase in the value of  $\alpha$ ,  $\sigma$ ,  $t$  and decrease with the increase in the value of  $R_w$  in both parent and daughter arteries.

## References

- [1] Young DF. Effect of a time-dependent stenosis on flow through a tube. *J Manuf Sci Eng* 1968;90:248–54.
- [2] Stokes VK. Couple stresses in fluids. *Phys Fluids* 1966;9:1709–15.
- [3] Stokes VK. Theories of fluids with microstructures. New York: Springer; 1984.
- [4] Srinivasacharya D, Srikanth D. Effect of couple stresses on the pulsatile flow through a constricted annulus. *CR Mecanique* 2008;336:820–7.
- [5] Sahu MK, Sharma SK, Agrawal AK. Study of arterial blood flow in stenosed vessel using non-Newtonian couple stress fluid model. *Int J Dynam Fluids* 2010;6(2):248–57.
- [6] Hayat Tasawar, Awais Muhammad, Ambreen Safdar, Hendib Awatif A. Unsteady three dimensional flow of couple stress fluid over a stretching surface with chemical reaction. *Nonlinear Anal: Modell Control* 2008;17(1):47–59.
- [7] Maiti S, Misra JC. Peristaltic transport of a couple stress fluid: some applications to hemodynamics. *J Mech Med Biol* 2012;12:1250048, 21 pages.
- [8] Srinivasacharya D, Srikanth D. Steady streaming effect on the flow of a couple stress fluid through a constricted annulus. *Arch Mech* 2012;64(2):137–52.
- [9] Adhikary SD, Misra JC. Pulsating flow of a couple stress fluid in a channel with permeable walls. *Forsch Ingenieurwes* 2013;77:49–57.
- [10] Rana MA, Khan Nosheen Zareen. Effects of couple stresses and variable suction/injection on the unsteady MHD flow of an Eyring Powell fluid between two parallel porous plates. *Life Sci J* 2014;11(4s):105–12.
- [11] Reddy JVR, Srikanth D, Murthy SK. Mathematical modelling of couple stresses on fluid flow in constricted tapered artery in presence of slip velocity-effects of catheter. *Appl Math Mech* 2014;35(8):947–58.
- [12] Hayat T, Iqbal Maryam, Humaira Yasmin, Fuad Alsaadi. Hall effects on peristaltic flow of couple stress fluid in an inclined asymmetric channel. *Int J Biomath* 2014;7(8):1450057–1–1450057–34.
- [13] Adesanya SO, Makinde OD. Irreversibility analysis in a couple stress film flow along an inclined heated plate with adiabatic free surface. *Physica A* 2015;432:222–9.
- [14] Prakash Om, Makinde OD, Singh SP, Jain Nidhi. Effects of stenoses on non-Newtonian flow of blood in blood vessels. *Int J Biomath* 2015;8(1):1550010. <http://dx.doi.org/10.1142/S1793524515500102>, 13 pages.
- [15] Makinde OD. Asymptotic approximations for oscillatory flow in a tube of varying cross-section with permeable isothermal wall. *Rom J Phys* 2007;52(1–2):59–72.
- [16] Prakashand J, Makinde OD. Radiative heat transfer to blood flow through a stenotic artery in the presence of magnetic field. *Lat Am Appl Res* 2011;41(3):273–7.
- [17] Makinde OD, Acho TM, Sibanda P, Lungu EM. The bio-mechanics of atherosclerosis development. *CAMES* 2003;10(1):23–31.
- [18] Makinde OD. Laminar flow in a channel of varying width with permeable boundaries. *Rom J Phys* 1995;40(4–5):403–17.
- [19] Makinde OD. Collapsible tube flow – a mathematical model. *Rom J Phys* 2005;50(5–6):493–506.
- [20] Chakravarty S, Mandal PK. An analysis of pulsatile flow in a model aortic bifurcation. *Int J Eng Sci* 1997;35(4):409–22.
- [21] Chakravarty S, Mandal PK, Mandal A. Mathematical model of pulsatile blood flow in a distensible aortic bifurcation subject to body acceleration. *Int J Eng Sci* 2000;38:215–38.
- [22] Shit GC, Roy M. Pulsatile flow and heat transfer of a magneto-micropolar fluid through a stenosed artery under the influence of body acceleration. *J Mech Med Biol* 2011;11:643–61.



**Dr. D. Srinivasacharya** completed Ph.D (Mathematics) at Regional Engineering College (N.I.T) Warangal, A.P., India, in the year 1996. His research interests are Fluid Mechanics, Computational Fluid Dynamics and Bio-Fluid Mechanics. He published about 120 papers in various reputed journals and supervised 11 Ph.D.s and guiding for 5 more. He completed 4 research projects and reviewed research articles in various national and international journals.



**G. Madhava Rao**, is pursuing Ph.D. (Mathematics) at National Institute of Technology, Warangal, A.P., India. His research interest is Bio Fluid Mechanics.